

REPORT



Epitope mapping of monoclonal antibodies: a comprehensive comparison of different technologies

Xibei Dang^{a*}, Lars Guelen^{b*}, David Lutje Hulsik^b, Grigori Ermakov^a, Edward J. Hsieh^a, Joost Kreijtz^b, Judith Stammen-Vogelzangs^b, Imke Lodewijks^b, Astrid Bertens^b, Arne Bramer^b, Marco Guadagnoli^b, Alexis Nazabal^c, Andrea van Elsas^b, Thierry Fischmann^a, Veronica Juan^a, Amy Beebe^a, Maribel Beaumont^{a#}, and Hans van Eenennaam^{b#}

^aPharmacokinetics, Merck & Co. Inc, Kenilworth, NJ, USA; ^bResearch, Aduro Biotech Europe, Oss, The Netherlands; ^cMedical, CovalX AG, Zürich, Switzerland

ABSTRACT

Monoclonal antibodies have become an important class of therapeutics in the last 30 years. Because the mechanism of action of therapeutic antibodies is intimately linked to their binding epitopes, identification of the epitope of an antibody to the antigen plays a central role during antibody drug development. The gold standard of epitope mapping, X-ray crystallography, requires a high degree of proficiency with no guarantee of success. Here, we evaluated six widely used alternative methods for epitope identification (peptide array, alanine scan, domain exchange, hydrogen-deuterium exchange, chemical cross-linking, and hydroxyl radical footprinting) in five antibody-antigen combinations (pembrolizumab+PD1, nivolumab+PD1, ipilimumab+CTLA4, tremelimumab+CTLA4, and MK-5890+CD27). The advantages and disadvantages of each technique are demonstrated by our data and practical advice on when and how to apply specific epitope mapping techniques during the drug development process is provided. Our results suggest chemical cross-linking most accurately identifies the epitope as defined by crystallography.

ARTICLE HISTORY

Received 2 November 2022
Revised 22 October 2023
Accepted 15 November 2023

KEYWORDS

Alanine scan; cross-linking; Epitope mapping; Hydrogen deuterium exchange; hydroxyl radical footprinting; monoclonal antibodies

Introduction



Over the last 35 years, monoclonal antibodies have become an important class of therapeutics for treatment of cancer, autoimmune disorders and infectious diseases, and more recently other disease areas such as cardiovascular and neuroscience. The market for antibodies exceeded global sales of 100 billion USD in 2018,¹ and recently antibodies reached another milestone with the 100th therapeutic being approved by the US Food and Drug Administration (FDA).²

During antibody development, selection of the right antibody that binds to the right domain is crucially important to obtain optimal therapeutic efficacy and engagement of the proposed mechanisms of action. For neutralizing or blocking characteristics, antibodies are usually selected to bind an epitope that lies in or close to the interface between receptor and ligand. For agonist antibodies, an epitope homologous to a previously well-validated agonistic anti-mouse antibody can be selected, as demonstrated in the development of MK-4166.³ For antibody effector functions, targeting different epitopes on CD20 has been shown to differentially recruit complement to exert complement-dependent cytotoxicity (CDC) function,⁴ while epitope specificity and location can influence the level of antibody-dependent cell-mediated cytotoxicity (ADCC) induction.⁵ Furthermore, antibodies binding distinct epitopes

may differentially affect receptor heterodimerization, internalization, ligand binding and, ultimately, receptor functionality, as was demonstrated for the Her2-EGF receptor-ligand pair.⁶


The epitope also plays an important role in drug patents.⁷ Identification of the epitope and its correlation with functional properties of the antibody is frequently laid down in epitope claims, which assume that any antibody targeting the same epitope will have similar functional (therapeutic) properties. Based on the same structure–function relationship the epitope is also used to differentiate from prior art antibodies.⁷

With such a central role for the epitope in the development of therapeutic antibodies, many technologies for epitope identification have been developed over the past decades. Among those technologies, X-ray crystallography (X-ray) is regarded as the gold standard to identify with high accuracy the key interactions between antibody and individual amino acids of the antigen at atomic resolution. Current state-of-the-art application allows resolution of antigen bound to an antibody at up to 1.2 Å.^{8–10} However, obtaining a crystal structure for an antibody-antigen complex takes time (months), has a moderate chance of success (not all antibody-antigen complexes form crystals), and requires relatively large amounts of materials and specialty equipment and expertise. Therefore, alternative methods that apply strategies to mutate/modify the

CONTACT Maribel Beaumont  maribel.beaumont@merck.com  Pharmacokinetics, Merck & Co. Inc, 213 East Grand Avenue, South San Francisco, CA 94080, USA

*equally sharing first authors.

#equally sharing senior authors.

 Supplemental data for this article can be accessed online at <https://doi.org/10.1080/19420862.2023.2285285>

© 2023 Merck and Co. Published with license by Taylor & Francis Group, LLC.

This is an Open Access article distributed under the terms of the Creative Commons Attribution-NonCommercial License (<http://creativecommons.org/licenses/by-nc/4.0/>), which permits unrestricted non-commercial use, distribution, and reproduction in any medium, provided the original work is properly cited. The terms on which this article has been published allow the posting of the Accepted Manuscript in a repository by the author(s) or with their consent.

antigen, study regions of the antigen that are shielded by the antibody, or detect antigen–antibody crosslinking have been developed. In the context of therapeutic antibody development all these technologies have specific pros and cons, which have been highlighted in numerous publications and review articles.^{11–14} Here, using two immunoglobulin family members, PD-1 and CTLA-4, and one TNF receptor-superfamily member, CD27, as target proteins, we performed six widely used technologies: 1) peptide array (PepArr), 2) alanine scan (ALN), 3) domain exchange (DomX), 4) hydrogen-deuterium exchange (HDX), 5) chemical cross-linking (XL), and 6) hydroxyl radical footprinting (HRF), to identify the epitopes of four antibodies (pembrolizumab, nivolumab, ipilimumab, tremelimumab) that are approved by the FDA, and boseroimab (MK-5890), which is in clinical development. Comparing the results of this study to published data obtained with X-ray crystallography,^{15,16} where amino-acids within 4 Å of each other are considered contact residues, provides a comprehensive view on epitope mapping technologies and their position in the drug development process.

Results

Peptide array

Different settings were used to study the binding of antibodies to peptides derived from PD-1, CTLA4, or CD27. Inspired by the work of Bai and colleagues¹⁷ a biolayer interferometry assay (Octet Red96) was developed using biotinylated linear peptides coupled to streptavidin-coated sensors. Using chemical synthesis executed by Sigma, a set of peptides were designed and generated that covered the full extracellular domain of PD-1, with each peptide shifting one amino acid as compared to the previous peptide. Screening for binding of those peptides using pembrolizumab and nivolumab revealed specific-binding peptides, of which one of the nivolumab consensus sequences was previously identified by Wang et al.¹⁸ Identified peptides with their wavelength changes are listed in Table S5.

Based on this success and hypothesizing that this technology might work across other immunoglobulin receptor family members, we also followed a similar strategy with CTLA-4 and derived biotinylated linear peptides to identify the binding peptides of ipilimumab and tremelimumab antibodies. In contrast to PD-1, none of the peptides demonstrated specific binding by any of the two antibodies.

In the case of the CD27 antigen, use was made from an alternative technology and MK-5890 CD27 antibody was screened for binding to both linear and circular peptides following the Pepscan technology. A similar approach was followed as had been successfully applied by us for another TNF superfamily member, APRIL.¹⁹ However, no peptides were identified in this antigen–antibody pair.

In summary, the peptide array method uses either linear or circular peptides, presenting 10–20 amino acid overlapping portions of the antigen, to identify the binding region of the antibody by technologies such as enzyme-linked immunosorbent assay (ELISA). Peptide arrays only identified partial epitopes from 2 of 5 antigen–antibody pairs. Only the N-terminal

epitope within strand C was revealed with pembrolizumab +PD1 (Figure 1a, second panel). Two of the three regions of nivolumab binding to PD-1 were identified (Figure 1b, second panel): the N-terminal portion and middle portion containing S60 and E61. Peptide array did not reveal any epitopes for ipilimumab/tremelimumab+CTLA4, or MK-5890+CD27.

Alanine scan

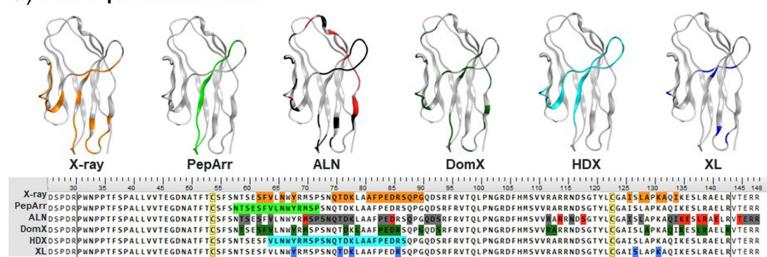
Alanine scanning is a protein engineering method where residues in the antigen are selected for substitution by alanine in either a model-guided or random approach. The interaction between amino acid sidechains of the binding surface is interrupted after substitution, thus the loss of antibody binding to the antigen is used as a measure to identify crucial amino acids. ALN identified partial epitopes from 3 out of 5 antigen–antibody pairs. With pembrolizumab+PD1 (Figure 1a, third panel), ALN revealed 10 residues (red residues) out of 37 tested (red + gray residues) as the epitope, but only one residue, D85, is part of the actual epitope as defined by crystallography and three residues (M70, K135 and E136) are adjacent to the identified epitope. The other six residues are too distantly removed from the epitope to form part of the binding region. We confirmed that these six substitutions do not affect PD-L1 and PD-L2 binding, suggesting that they do not grossly affect the conformation of the PD-1 protein and specifically the domain involved in PD-L1 and PD-L2 binding (data not shown). Furthermore, 12 residues identified by crystallography and tested by ALN had no binding loss (gray residues). Similarly with nivolumab (Figure 1b, third panel), ALN only revealed residues that are distantly removed from the binding region despite testing of multiple residues in or within close proximity to the X-ray epitopes. All four amino acids identified using ALN as important for MK-5890 binding (P28, H56, R57, K58) matched the epitope as resolved using crystallography (Figure 1e, second panel).

An important consideration is that alanine substitutions might alter the antigen structure, which, if not well controlled, can lead to the identification of false-positive epitope residues. As shown in Figure 3, many alanine substitutions resulted in the loss of CD80 and CD86 binding to the CTLA-4 protein, indicating that the CTLA-4 structure integrity is dependent on many single amino acids. This observation was found to be antigen-dependent. CD27 has a rigid structure with 8 intra-disulfide bonds, thus a single alanine mutation is unlikely to interrupt its folding and structure. Indeed, for CD27+MK-5890, ALN results correlate well with the X-ray data.

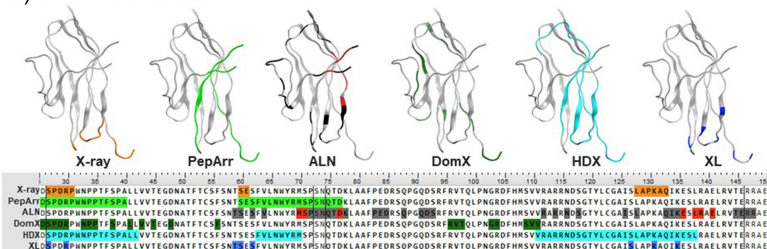
Domain exchange

A similar method to ALN, but less granular, is domain exchange, where structural domains or segments in the antigen are exchanged for equivalent structural elements derived from a homologous sequence. We were able to create human-mouse exchange mutants because the predicted structures of human and mouse proteins suggest similar folding, and the antibodies studied are not cross-reactive to the mouse antigen. Domain exchange was helpful in identifying antibody-binding domains for all antigen–antibody pairs (Figure 2). Pembrolizumab

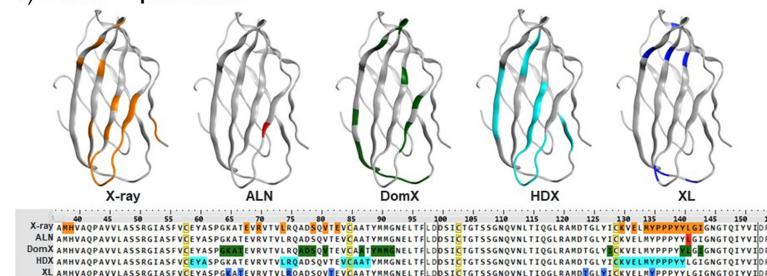
a) PD1 + pembrolizumab



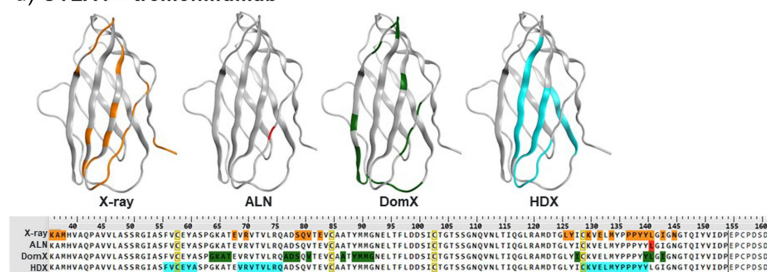
b) PD1 + nivolumab



c) CTLA4 + ipilimumab



d) CTLA4 + tremelimumab



e) CD27 + MK-5890

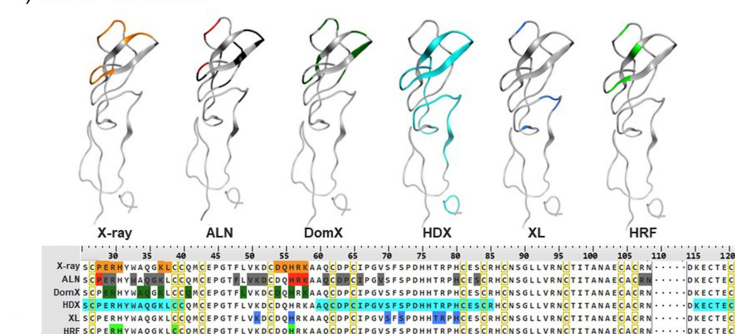


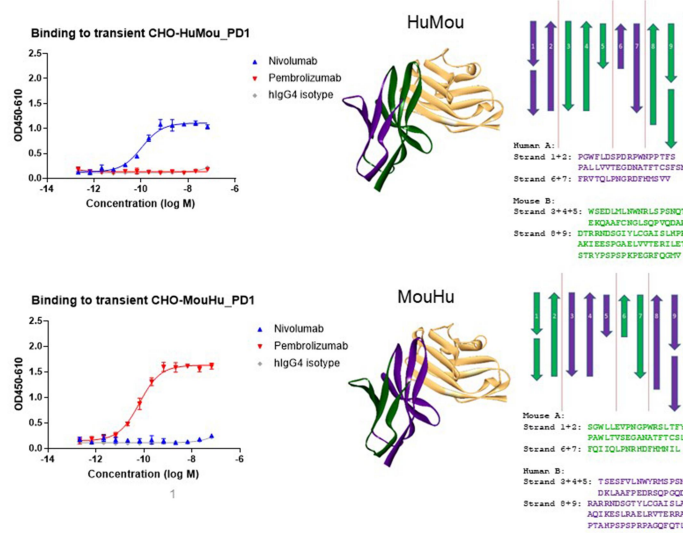
Figure 1. Binding epitopes of antigen-antibody pairs as determined by different technologies. The amino acids forming the binding epitopes of the antigen-antibody pairs, as identified by multiple epitope mapping technologies are highlighted on model structures of the antigens and their amino acid sequences. a) PD-1 + pembrolizumab. b) PD-1 + nivolumab. c) CTLA-4 + ipilimumab. d) CTLA-4 + tremelimumab. e) CD27 + MK-5890. X-ray: X-ray crystallography. PepArr: Peptide array. ALN: Alanine scanning; red residues resulted in loss of binding upon mutation while gray residues were mutated and showed negative result in ALN. DomX: Domain exchange. HDX: Hydrogen-deuterium exchange. XL: Chemical cross-linking. HRF: Hydroxyl Radical Footprinting.

binds to strands 3 + 4 + 5 + 8 + 9, while Nivolumab binds to the opposite strands 1 + 2 + 6 + 7. Both ipilimumab and tremelimumab bind to strands 3 + 4 + 7 + 8. For CD27, exchange

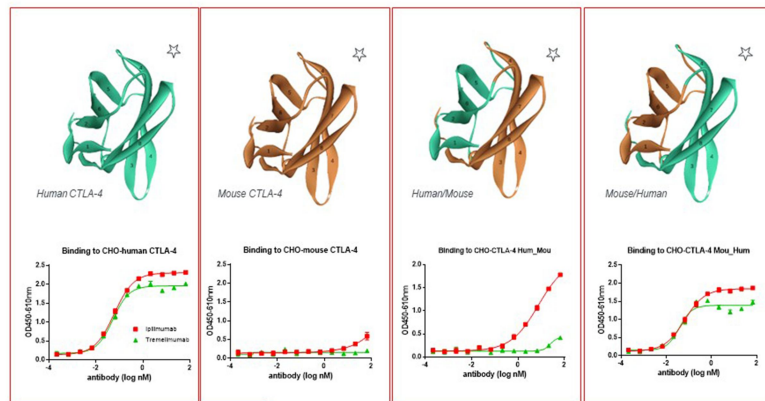
of the three human Cysteine-Rich Domains (CRDs) with individual mouse CRDs pointed toward binding to CRD1 for the MK-5890 antibody.

a) Exchange mutants mouse/human PD-1

Binding profile determined by cell ELISA



b) Exchange mutants mouse/human CTLA4



*All variants bind to CD80/CD86, indicating they are correctly folded

c) Exchange mutants mouse/human CD27

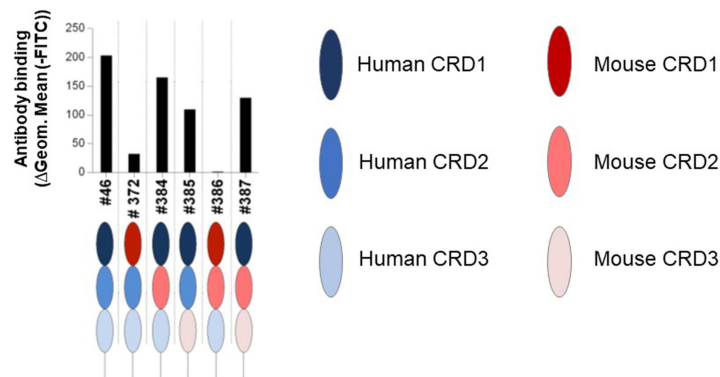


Figure 2. Antibody binding to mouse/human domain exchange mutants. Mouse/human exchange mutants were transiently transfected into CHO-K1 cells, after which antibody binding was determined. a) Binding of pembrolizumab and nivolumab to mouse/human PD-1 domain exchange mutants was determined by cell ELISA (left). The designs of the mutants are shown on the right. Purple represents human domains and green represents mouse domains. b) Binding of ipilimumab and tremelimumab to human CTLA-4, mouse CTLA-4 and CTLA-4 mouse/human exchange mutants was determined by cell ELISA. In ribbon drawings, green represents human domain and brown represents mouse domain. c) Binding of MK-5890 to CD27 mouse/human domain exchange mutants, as established by FACS. Human CRDs are indicated in blue, mouse CRDs in red.

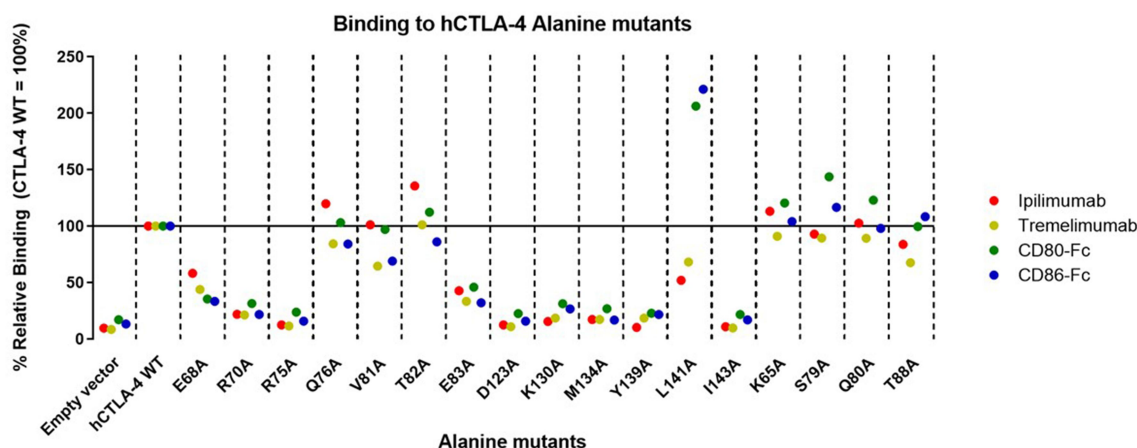


Figure 3. Binding of anti-CTLA-4 antibodies to alanine mutants. Single amino acids of CTLA-4 were mutated into alanine and mutant proteins were expressed on CHO-K1 cells. Binding of ipilimumab, tremelimumab and the CTLA-4 ligands CD80 and CD86 is expressed relative to antibody binding to wild type hCTLA-4 (hCTLA-4WT), which was set at 100%. Amino acid positions of the alanine substitutions are indicated.

Once differential binding between domain mutants has been found, residues that are potentially part of the binding epitope can be identified by aligning the human and the mouse protein sequences. With PD1+ pembrolizumab, DomX provided epitopes that are well aligned with X-ray (Figure 1a, fourth panel). However, with a different antibody (nivolumab) for the same antigen, DomX mostly pin-pointed residues that are distant from those identified by X-ray (Figure 1b, fourth panel). This is because only residues that are naturally different between human and mouse can be identified by DomX, and these may not be the ones that play a role in the observed loss of binding. Thus DomX results must be confirmed by another method.

Hydrogen-Deuterium Exchange (HDX)

Hydrogen-deuterium exchange (HDX) is a mass spectrometry-based epitope mapping technique.²⁰ When in deuterium buffer, the hydrogen of the amide bonds from the antigen backbone can exchange with the deuterium in the solvent, resulting in a mass increase. The speed of such exchange depends on the local conformation and dynamics and can be captured with a time-course experiment to characterize the local environment of a folded protein. Upon binding to the antibody, the amide hydrogen on/near the binding surface will be protected from the solvent, resulting in less deuterium uptake, thus less mass shift. HDX yielded results for all 5 antigen-antibody pairs. HDX data show overlap with X-ray results, except for missing the C-terminal residues for pembrolizumab+PD1 and the D54-K58 region for MK-5890+CD27 (Figure 1 and Figure S1-S5).

Compared with crystallography, HDX generally revealed larger binding regions. Although nonspecific enzymes like pepsin and protease XIII were used for digestion to generate overlapping peptides, the resolution is still limited to the peptide level, which can result in “overestimation” of epitopes, as observed with PD1+nivolumab, for which the identified regions account for about 40% of the PD-1 antigen. The resolution of HDX is closely related to the digestion efficiency of the antigen, which is heavily dependent on the antigen’s

structure and sequence. As mentioned above, CD27 is tightly locked between 8 intra-molecular disulfide bonds, which greatly limits the number of peptides that can be generated, resulting in non-ideal HDX results. Another difference between HDX and X-ray/ALN/PepArr/XL/DomX is that HDX measures “protection” rather than “binding” (similar to HRF, which also measures protection). Allosteric conformational changes upon binding that result in reduced solvent exposure will be identified by HDX as “epitope” as well. Without structure/modeling or another orthogonal method, HDX by itself does not yield definitive epitope information, although a good estimate can be made. However, the ability to measure conformational changes can also be an advantage. For example, conformational structure change in PKG Ia induced by cGMP activation has been measured by HDX.²¹

Hydroxyl radical footprinting

Hydroxyl radical footprinting (HRF) is another mass spectrometry-based epitope mapping technique. Hydroxyl radicals are generated in solution for a short period of time (several milliseconds) and oxidize the side chains of the amino acid residues. The short half-life of the hydroxyl radicals ensures the integrity of the protein structure and only introduces limited oxidation to the side chains. Similar to HDX, the rate of reaction is determined by solvent accessibility. However, the modification on the amino acid residues is irreversible and thus can be identified and localized through proteolysis followed by MS/MS fragmentation, providing residue resolution for epitope mapping. Hydroxyl radicals react with the side-chains of 14 different amino acids,^{22,23} thus HRF could underestimate the epitope due to the limited availability of reactive side chains at the epitope. Only the pair of CD27+MK-5890 was tested for HRF, and the four amino acid residues identified with HRF (R30, H31, C39, H56) are well aligned with the binding sites identified in the X-ray crystal structure (Figure 1e, sixth panel). HRF shares many attributes with HDX. It measures binding between antigen and antibody in a dynamic, soluble environment. The results show the “protection” of the antigen from the solvent upon antibody binding,

rather than the “binding” itself. One difference between HRF and HDX is that the labeling in HRF is non-reversible so back-exchange will not be a concern.

Chemical cross-linking

Chemical cross-linking (XL) induces stabilized covalent bonds between amino acid sidechains within noncovalent protein complexes. Similar to HRF, the amino acid residues that are linked by the chemical linker can be identified by enzymatic digestions followed by LC-MS/MS. Numerous labeling reagents have been developed and applied. The chemical cross-linker used in this study is disuccinimidyl suberate (DSS), with reactivity to 6 amino acid residues (Lys, His, Ser, Thr, Arg, Tyr) and a linker length of 10–12 Å. DSS labels residues that are within 3 AA distance of the binding site. XL provided results for all 4 antigen–antibody pairs tested and by far provides the best alignment to X-ray data. All residues identified by XL are in or within close proximity to the epitope, except for the S70–S72 and T77–H80 region of CD27 (Figure 1).

In contrast to some of the other technologies, XL can be more readily used to identify residues of the antibody that crosslink with the antigen, the so-called paratope. As listed in Table 1, four technologies are capable of paratope mapping, namely X-Ray, HDX, HRF, and XL. And with XL, aside from X-ray, paratope can be generated automatically as a side product of epitope mapping, with no additional experiment or data analysis needed. For HDX and HRF, to map paratope, one needs to add in one control experiment with the antibody itself, and analyze the data separately. XL revealed that similar residues were found to form the binding interface between antibody and antigen as demonstrated by crystallography (Figure 1 and Table S1).

Detailed comparison of the binding regions reveals that XL may “underestimate” the epitope. Where continuous-binding regions are identified using crystallography, individual amino acids (‘touchpoints’) are identified with XL. One reason for the “underestimation” is the limited reactivity of the linker to only 6 amino residues. In the case of ipilimumab, the stretch of M134 to I143 near the C-terminus of CTLA4 is identified as epitope by X-ray, yet only Y135 is reactive to be labeled by XL. Similarly, for PD-1 + pembrolizumab, within the X-ray epitope spanning A81 to G90, only R86 can be labeled. This “underestimation” of epitopes has also been reported by other researchers. One study from the Gross lab identified 5 cross-linked amino acid residues for the PD-1 and nivolumab pair, namely D26, S27, E61, S62, and K131. Those residues mostly overlap with our assigned residues (S27, R30, T59, S60, S62, S127, K131, and K135) for the same antibody and antigen pair¹¹. Also, the residues on both sides of the binding surface need to maintain a certain distance to be crosslinked. If the residues are too well protected, XL will miss them due to the limited solvent accessibility of the residues and the steric hindrance caused by the limited space between them. For example, with pembrolizumab+PD-1, XL did not identify antibody complementarity-determining region 3 (CDR3) residues in the heavy and light chain (Table S1). And with ipilimumab+CTLA4, XL missed R70, S79, Y139, and Y140. Thus, the identified residues by XL would form a ring around the binding surface, which can be most easily seen in Figure 1c, 5th panel with ipilimumab. Table S1 summarizes all epitope-paratope pairs with the distance between alpha-carbons calculated. The distance is mostly between 15 and 30 Å, in agreement with similar studies²⁴. Overall, even with the mentioned limitations, XL provides a clear interaction interface between antibody and antigen, where other technologies are less reliable.

Table 1. Pro and cons of each technique.

Technique	X-Ray	HDX	HRF	XL	ALN	PepArr	DomX
Speed	Slow (months)	Fast (2–4 weeks)	Fast (4–6 weeks)*	Fast (3–5 weeks)	Fast (3–6 weeks)**	Slow (1–3 month)	Fast (4–6 weeks)
Material Used	~20 mg	0.5–1 mg	0.5–1 mg	~0.2 mg	Transient transfection	20–100 µg antibody	Transient transfection
Resolution	Atomic	Peptide	Residue	3 AA	Residue	Peptide /Residue	Domain /Residue
PTM tolerance	Very low	Moderate-High	High	High	Native PTMs	Absent	Native PTMs
Cost	\$\$\$	\$\$	\$\$	\$\$	\$	\$	\$
Throughput	Single	Several	Several	Several	Several	Multiple	Multiple
Access to technology	Specialist	Broad	Specialty CRO	Broad/CRO	Broad	Broad/CRO	Broad
Paratope Mapping	Yes	Low res	Yes	Yes	No	No	No
Linear or conformational	Conformational	Conformational	Conformational	Conformational	Conformational	Linear	Conformational
Epitope							
Structural or functional	Structural	Structural	Structural	Structural	Functional	Functional	Functional
Epitope							
Notes	No guaranteed output	Measures “protection” upon binding	Measures “protection” upon binding. 12+ out of 20 AA can be targeted.	Only crosslinks 6 out of 20 AA	Mutations can compromise antigen folding and function	Linear epitope mostly	Structure should be available

*Subject to synchrotron availability.

**Longer for soluble antigen.

Discussion

The six epitope mapping technologies used here can be divided into two groups. HDX, HRF, and XL are structure-based methods while ALN, Peptide Array, and DomX are function (binding) based methods. The pros and cons of each technology, with the addition of X-Ray and BioNMR, are summarized in Table 1.

The three function-based methods, DomX, Peptide Array and ALN, provide strand-level, peptide-level, and residue-level resolution, respectively. Peptide array had the lowest success rate among all technologies tested here. Although it has been successfully applied with antigens like Her2⁶, APRIL¹⁹, and PD-1, Peptide Array was not successful for CTLA-4 targeting antibodies or MK-5890. Based on the x-ray analyses one would, with the limited data available, be able to suggest that using linear peptide arrays will only reveal larger, spatial, rather than more complex, more distributed and conformational epitopes. This is furthermore supported by our previous work using Pepsan peptide arrays that identified a quite linear epitope for the anti-APRIL antibody¹⁹ and the lack of identification of binding region for MK-5890 (conformational epitope). The low probability of success, the apparent limited epitope coverage, and low resolution are clearly a downside of this approach.

The value of DomX is its high success rate at producing high-level mapping results, which can be cross-validated with other methods and used to guide residue selection in ALN. This technology has also been used to map the epitopes of Her2,⁶ followed by validation using a peptide-based epitope scanning method. Based on the collective data presented here, we regard this approach only relevant when clearly defined and isolated domains can be interchanged. Especially when multiple domains can be identified within the target protein, exchanging domains becomes more informative. In addition, results are easier to interpret when model systems are used that are either positive or negative for binding of the antibody rather than displaying intermediate/weaker binding to both proteins. Here, we present the exchange of immunoglobulin or TNF-receptor family members and both proved to be partially suitable for this approach. In all cases, it required well established controls to establish the integrity of the overall conformation and impact of mutation on the expression level on the membrane.

Higher resolution may be obtained using ALN, but only some residues within the epitope were identified that completely abrogated binding of the antibody to the antigen. This does not indicate that the antibody only binds to those amino acids, but merely points to the fact that substituting one amino residue at a time can be insufficient to abrogate the binding. Substitution of two or more amino acids may give a more precise view on the larger binding sites. On the other hand, with the PD-1 + pembrolizumab and PD-1 + nivolumab pairs, there are several false positive residues identified with ALN. Our hypothesis based on the obtained data is that, although the overall conformation as established by positive ligand binding is not affected by the false positive alanine mutations, more

subtle changes that do not impact the ligand binding might cause the antibodies not to bind anymore. For example, alanine substitution may result in distortion of the loop immediately adjacent to the binding epitope that might affect the binding of the antibody. In addition, certain false positives might result in distortion of the shape of a part of the immunoglobulin domain, resulting in loss of binding.

ALN is a relatively fast method when the antigens are expressed on the cell surface and their binding is measured by FACS. However, for soluble antigens, e.g., cytokines, the required purification and characterization of antigens makes it much more time consuming and results in lower throughput.

XL, HDX, and HRF are all structure-based epitope mapping methods. All three technologies show a high probability of success and have no limitation of antigen size. All technologies require costly high-resolution mass spectrometry and specialized expertise, but can be done by contracted companies. HDX is the best commercialized technology with a fully automated instrumental system and easy to use commercial software packages. HDX suffers most from its mid-low peptide level resolution. This limitation is consistent with HDX results from other research. One study from the Gross lab identified three protected peptides for the PD-1 and nivolumab pair, namely LDSPDRPWNPTFSPALL (25–42), AAFPEDRSQPGQDCRF (80–95), and AISLAPKAQIKESL (125–138). Those regions mostly overlap with our assigned protection regions (SPDRPWNPTFSPALL (27–42), FVLNWYRM (63–70), and VRARRNDSGTYLCGAISLAPKAQIKESL (111–138)) for the same antibody and antigen pair.¹¹ However, the recent introduction of electron transfer dissociation (ETD) and ultraviolet photodissociation (UVPD) into the workflow with minimal gas phase scrambling may significantly improve the resolution of HDX by fragmenting the peptides in the mass spectrometer to measure residue-level deuterium uptake.^{25–27} Also protein docking software like HADDOCK can combine HDX data and modeling to achieve more defined epitope mapping.²⁸

HRF shares similar attributes with HDX, but with covalent labeling on the side chain and higher resolution. One key factor for a successful HRF experiment is to control the exposure time of the protein to the hydroxyl radical (under 30–50 milliseconds) to keep the oxidation level to less than 30%.²³ Over-exposure to the hydroxyl radical compromises the structural integrity of proteins and can result in protein aggregation and cleavage. Synchrotron X-ray radiolysis is by far the best method for generating hydroxyl radicals for HRF, because the reaction time is precisely controlled by the duration of the laser pulse, and no reagents other than water are needed, providing a physiological condition for the proteins. However, the method is limited by the availability of synchrotron X-ray sources, which may cause a delay of months before an HRF experiment can be conducted. Limited oxidation of proteins can be achieved with laser photolysis, or fast photochemical oxidation of proteins (FPOP) using H₂O₂ as reagent, laser as energy source, and a chemical scavenger for quenching. HRF has not been automated and no commercial platforms or software packages are available, but it is a fast-growing technology; reagents and platforms are under rapid

development.^{29,30} However, neither HDX nor HRF provide definitive epitope mapping because their results cannot differentiate conformational changes from binding. Thus, another method, either XL or a function-based approach, is needed for cross-reference.

XL is the most reliably predicted antibody binding regions in our study. It generates data relatively quickly, with less material and at lower expense. In the case of CD27 and the MK-5890 antibody, XL revealed a second region of interaction which was not captured by X-ray. This additional region is too far apart to physically interact with the CDRs of the antibody and, at the same time, the length of the crosslinking spacer is insufficient to bridge between the antibody bound to the first epitope and this second region (S70-S72 & T77-H80). The observation from XL that this second epitope interacts with LC-CDR2, HC-CDR2, and HC-CDR3 of the antibody ('paratope') suggest that this may be a true interaction rather than an artifact. An explanation might be that the CD27 protein has a dynamic structure and can undergo a conformational change, whereby the second domain comes within the distance to allow crosslinking. Support for this hypothesis is found in HDX data, and some moderate protection observed in HRF (Table S3). This points out a critical difference between crystallography versus XL, HDX, and HRF, where the former method detects binding in a crystalline state. The suggested dual-binding mode of the MK-5890 antibody might explain the unique capability of the antibody to activate CD27 signaling without the need for crosslinking. Similarly, a direct link between a conformational change and receptor activation has been described for AMPA glutamate receptors.³¹

Although not tested here, BioNMR comes with many features that are similar to crystallography: atomic resolution, single throughput and requirement for extensive specialist expertise. However, it has a lower success rate, requires labeled protein material, and generally works with proteins under 25 kDa.^{32,33} On the other hand, Cryo-EM has been gaining momentum in the realm of epitope mapping.³⁴

In this study, we provided a unique comparison of different technologies/applications that are commonly used to map the epitope of antibodies. Although no technology could identify the interaction points between antibody and antigen at the atomic or even amino acid level as well as crystallography, the alternative technologies did estimate the binding surface and epitope at a lower cost with a higher likelihood of generating results quickly. Among all technologies we tested, XL provided results that overlapped best with X-ray data for all 4 antigen-antibody pairs tested. HDX and HRF are also technologies with high success rates, although their results are slightly less ideal, overestimating or underestimating the results, respectively (see Results section). DomX in combination with ALN could yield reasonable results when mouse and human structure are comparable and antibodies tested do not bind to the mouse protein. Peptide Array yields the poorest results both in terms of success rate and resolution.

Based on the limitations discussed, each method has potential use at different times in development. Initially, a crude mapping of the binding region (DomX, Peptide Array, HDX) can be used to prioritize antibody candidates (so-called epitope binning) and start intellectual property

filing. At a later stage of drug development, atomic, or residue resolution (X-ray, HRF, XL, ALN) is functionally important to guide affinity maturation, removal of post-translational modifications, and to understand the basis for the functional activity the antibody unleashes when binding to the target protein. Importantly, this information is also used during prosecution of patent applications, where binding regions linked to the functional activity (mechanism of action) of antibody forms the basis either to claim a position or to differentiate from prior art antibodies.

Materials and methods

Protein sequences and structures

Protein sequences of human PD-1 (UniProt ID: Q15116), mouse PD-1 (Q02242), human CTLA-4 (P16410), mouse CTLA-4 (P09793), human CD27 (P26842), and mouse CD27 (P41272) were from Uniprot database. Protein structure PD-1 (PDB ID: 3RRQ), CTLA-4 (PDB ID: 3BIK), and CD27 (PDB ID: 5TLK) were from the PDB database and used in all experiments.

Protein sourcing and QC

Protein used in this manuscript, their type, sequence, source, expression system, purity and QC method is summarized in Table S4.

Single residue alanine substitution mutant design

The accessible surfaces of the protein structures of PD-1 (PDB ID: 3RRQ), CTLA-4 (PDB ID: 3BIK), and CD27 (PDB ID: 5TLK) were determined using Discovery Studio 4.1 using default parameters. Preferably residues with an exposed sidechain surface were selected for alanine substitution. The alanine substitution mutants of hCD27, hPD-1, and hCTLA-4 were generated by site-directed mutagenesis (Agilent). Mutant sequences were confirmed by DNA sequencing (Macrogen).

Single residue alanine substitution mutant expression

hPD-1, hCTLA-4 or hCD27 alanine substitution mutants was expressed using CHO-K1 cells, transiently transfected with pCI-neo empty vector, pCI-neo encoding wildtype targets, or pCI-neo encoding the mutant targets. CHO-K1 cells were first trypsinized, counted and seeded at a density of 1.0×10^5 per well in the DMEM/F-12 medium (Gibco cat.no. 11320) with 5% Hi Filtered bovine serum (fortified calf) (Hyclone, cat.no. SH30414.02) and 1% pen/strep (Gibco, cat. no. 15140). Cells were incubated 3 days at 37°C, 5% CO₂. Transfections were carried out in 6-well plates with 4 µg plasmid DNA and 10 µl Lipofectamine 2000 Reagent per well, both diluted in OPTI-MEMI, according to the manufacturer's instructions. The transfected cells were then incubated for one day at 37°C and 5% CO₂ in a humidified incubator.

Antibody binding to single residue alanine substitution mutant by FACS

After one day incubation, the transfected cells were washed once in Dulbecco's phosphate-buffered saline (DPBS), detached with 400 μ l enzyme-free cell dissociation solution (Gibco 13,151-014) and collected in 800 μ l ice-cold MACS buffer (Miltenyi Biotec, 130-091-221). Detached cells were transferred to 96-well, round-bottomed plates at approximately 1.2×10^5 cells/well. After spinning down the cells, discarding the supernatants and re-suspending the cells in the residual volume, the primary antibodies were added and incubated for 30 min at 4°C. Cells were washed three times with DPBS/bovine serum albumin (BSA) 1%, followed by centrifugation, discarding of the supernatants and re-suspension in the residual volume. Binding of the primary antibodies was detected by staining for 30 minutes at 4°C with goat-anti-mouse IgG-FITC (BD Bioscience 349,031, 2 μ l/well) or goat-anti-human IgG-FITC (γ -chain specific, Southern Biotech, 2040-02, 2 μ l/well). After washing once, antibody binding was detected using the HTS plate reader (FACS Canto II) and FlowJo software for data analysis. Debris, dead cells, and doublets were excluded from the analysis. Expression of the mutants was confirmed using the natural ligand or a polyclonal antibody.

Exchange mutant design

PD-1 and CTLA-4

Protein structures of human PD-1 (PDB ID: 3RRQ) and mouse PD-1 (3BIK) were aligned in Discovery Studio 4.1, using default parameters. The structural alignment was used to determine the two sheets into which the PD-1 protein could be divided. Sheet A contains beta strands 1, 2 (residues 21–58), 6 and 7 (95–111). Sheet B contains beta strands 3, 4, 5 (59–94), 8 and 9 (112–170). Two constructs were designed; one composed of mouse sheet A and human sheet B, including human transmembrane and intracellular domains, and one composed of human sheet A and mouse sheet B, including mouse transmembrane and intracellular domains. Structural alignment of human CTLA-4 (3OSK) and mouse CTLA-4 (1DQT) showed that the protein could be divided into two sheets: sheet A, containing beta strands 1, 2 (36–63), 5 and 6 (93–122), and sheet B, containing beta strands 3, 4 (64–92), 7 and 8 (123–161). Two constructs were designed, one composed of mouse sheet A and human sheet B, and one composed of human sheet A and mouse sheet B. Both constructs were designed with human transmembrane and intracellular domains. Constructs were back translated into codon optimized expression constructs and synthesized.

CD27

Protein sequence alignment of human CD27 and mouse CD27 was performed using CLUSTALO. High sequence similarity (71.4%) in cysteine-rich domains 1 to 3 predicted high structural similarity, allowing exchange of the CRD1 to 3 and combinations thereof between human and mouse CD27. Five exchange constructs were designed. Constructs were back translated into codon optimized expression constructs and synthesized.

Exchange mutant expression

PD-1, CTLA-4, and CD27 domain exchange mutants were expressed using CHO-K1 cells, transiently transfected with pCI-neo empty vector, pCI-neo encoding the wildtype target, or pCI-neo encoding the exchange mutants. CHO-K1 cells were first trypsinized, counted and seeded at a density of 1.0×10^5 per well in the DMEM/F-12 medium (Gibco cat.no. 11320) with 5% Hi Filtered bovine serum (fortified calf) (Hyclone, cat.no. SH30414.02) and 1% pen/strep (Gibco, cat. no. 15140). Cells were incubated 3 days at 37°C, 5% CO₂. For PD-1 and CTLA-4 exchange mutants, transfections were carried out in 24-well plates with 0.8 μ g plasmid DNA and 2 μ l Lipofectamine 2000 Reagent (Invitrogen 11,668-019) per well, both diluted in OPTI-MEMI (Gibco, cat.no. 31985), according to the manufacturer's instructions. And the transfected cells were incubated for one day at 37°C and 5% CO₂ in a humidified incubator. For CD27 exchange mutants, Transfections were carried out in 6-well plates with 4 μ g plasmid DNA and 10 μ l Lipofectamine 2000 Reagent per well, both diluted in OPTI-MEMI, according to the manufacturer's instructions. And the transfected cells were incubated overnight at 37°C and 5% CO₂ in a humidified incubator.

Antibody binding to mouse/human domain exchange mutants by FACS

For PD-1 and CTLA4 exchange mutants, 100 μ l antibody solution was diluted in culture medium and added to each well. Cells were incubated with the antibody solution for 1 h at 37°C. Next the cell culture plates were washed 3 times using an ELISA washer with a solution of phosphate-buffered saline (PBS) supplemented with 0.02% Tween20. Next, 100 μ l/well Goat anti-human IgG-HRP conjugate (Jackson ImmunoResearch, cat.no.109-035-088, C038) was added, followed by 1 hour incubation at 37°C. The plates were washed 3 times using the ELISA washer with the PBS/0.02% Tween20 solution, 100 μ l/well TMB substrate (Invitrogen, cat.no. SB02) was added and plates were incubated for 10 min at room temperature. The reaction was stopped by addition of 100 μ l/well 0.5 M H₂SO₄. Signal intensities were measurement using the A450 – A620 ratio on the Envision plate reader (PerkinElmer)

For CD27 mutants, cells were washed once in Dulbecco's phosphate-buffered saline (DPBS), detached with 400 μ l enzyme-free cell dissociation solution (Gibco 13,151-014) and collected in 800 μ l ice-cold MACS buffer (Miltenyi Biotec, 130-091-221). Detached cells were transferred to 96-well, round-bottomed plates at approximately 1.2×10^5 cells/well. After spinning down the cells, discarding the supernatants and re-suspending the cells in the residual volume, the primary antibodies were added and incubated for 30 min at 4°C. Cells were washed three times with DPBS/BSA 1%, followed by centrifugation, discarding of the supernatants and re-suspension in the residual volume. Binding to MK-5890 was detected by staining for 30 min at 4°C with goat-anti-mouse IgG-FITC (BD Bioscience 349,031, 2 μ l/well) or goat-anti-human IgG-FITC (γ -chain specific, Southern Biotech, 2040-02, 2 μ l/well). After washing once, antibody binding was

detected using the HTS plate reader (FACS Canto II) and FlowJo software for data analysis. Debris, dead cells, and doublets were excluded from the analysis. Expression of the mutants was confirmed using the natural ligand or a polyclonal antibody.

Peptide array/octet

PD-1 Peptide sequences used in the peptide array were summarized in Table S5. Peptides were designed with a frame-shift of one amino acid difference, covering the whole extracellular domain of PD-1. All peptides using in the study were chemically synthesized by a commercial vendor (Sigma) and were quality controlled by HPLC.

Binding of anti-PD-1 antibodies to PD-1 peptides was measured by biolayer interferometry using an Octet RED96 instrument (ForteBio). Sixty-four overlapping peptides spanning the entire extracellular domain of human PD-1 were synthesized and biotinylated at their NH₂-termini (Sigma Aldrich) (Table S6). PD-1 peptides (1 μ mol/L) and a negative control peptide (1 μ mol/L) were captured on streptavidin Octet biosensors. Sensorgrams were recorded when peptide-loaded biosensors were incubated with antibody (1 μ mol/L) in Octet sample diluent. Baseline was established by incubating the peptide-loaded biosensors with an antibody diluent. Change in wavelength was compared to baseline, referred to in response unit of > 0.1 were set as threshold for positive binding signal.

Hydrogen-deuterium exchange mass spectrometry

Hydrogen-deuterium exchange mass spectrometry (HDX-MS) was performed by incubating antigen with the antibody in phosphate buffered saline composed of 99% deuterium oxide (Cambridge Isotope Laboratories). An antigen-only control sample was generated by substituting the antibody with phosphate buffered saline. After incubating for labeling times of 30–12000 s, the samples were quenched with chilled, low pH solution (8 M Urea, 100 mM Tris (2carboxyethyl) phosphine). Each time point was measured in triplicate. A fully deuterated control sample was prepared by incubating antigen in deuterated, denaturing buffer (4 M Urea, 100 mM Tris (2-carboxyethyl) phosphine, 99.5% deuterium oxide) overnight at room temperature.

The quenched samples were injected over a chilled immobilized pepsin/protease type 13 column (XIII/pepsin 1:1, NovaBioassays) that was placed in line with a C18 reverse phase trap (Vanguard CSH C18 pre-column). The resulting peptides were analyzed by liquid chromatography-mass spectrometry with Acquity Peptide CSH C18 Column using a nanoAcquity coupled Orbitrap Elite. The level of deuterium incorporation into peptides was calculated (HDEaminer, Sierra Analytics). First, HDEaminer ignores the first two residues of each peptide since these are widely considered to exchange too rapidly to be useful. The software then divides the protein into non-overlapping “atomic peptides”. These atomic peptides are formed by dividing the protein everywhere an observed peptide starts or ends. Each observed peptide’s deuteration level can then be expressed as a sum of deuteration levels for one or more atomic peptides. HDEaminer

computes a deuteration level for each atomic peptide that minimizes the least squares error with the set of observed peptides. The antibody epitopes were determined by comparing deuterium incorporation of the control and the antibody incubated samples based on the heat map generated by the software. Deuterium uptake difference of 10% was considered as a cutoff value. In these experiments, antibody paratopes were not measured since the peptide-level resolution of HDX would offer little more information than the CDRs already known from the antibody sequence.

Hydroxyl radical footprinting

For footprinting experiments, both the mAb and CD27 antigen proteins were buffer exchanged into 1×PBS buffer, pH 7.4 using Amicon 3K filters. The free antigen sample was prepared with a final protein concentration of 6 μ M. The mAb-antigen complex was formed using 1:2 mAb:antigen molar ratio resulting in a final protein concentration of mAb and antigen in the complex of 3 and 6 μ M, respectively. All samples were exposed to hydroxyl radicals for intervals of 0, 10, 25, and 50 milliseconds using the X-ray beam line at the ALS, Berkeley National Laboratory. Next, all irradiated samples were reduced and alkylated with 10 mM and 25 mM of DTT and iodoacetamide, respectively. Subsequently, all samples were subjected to dual digestion with 1000 ng Lys-C (1:10 enzyme to protein ratio) for 1 hr at 37°C, and overnight at 37°C with 1000 ng trypsin (1:10 enzyme to protein ratio), followed by liquid chromatography coupled with high-resolution mass spectrometry (LC-MS). The MS data was analyzed manually, resulting in dose-response plots for each peptide. Results from the free CD27 antigen were compared against the antigen-mAb complex form.

Cross-linking

Prior to crosslinking the complex, both antibody and antigen were incubated separately with crosslinkers and aggregation levels were checked using a Ultraflex III MALDI ToF mass spectrometer (Bruker) equipped with a HM4 interaction module. Next, 20 μ L of the Antibody/Antigen mixture at 0.33–0.6 μ M/1.5 μ M concentration were mixed with 2 μ L of DSS d0/d12 (2 mg/mL; DMF) before 180 minutes incubation time at room temperature. After incubation, the reaction was stopped by adding 1 μ L of Ammonium Bicarbonate (20 mM final concentration) before 1 h incubation time at room temperature. Then, the solution was dried using a speedvac before H₂O 8 M urea suspension (20 μ L) was added. After mixing, 2 μ L of DTT (500 mM) was added to the solution. The mixture was then incubated 1 hour at 37°C. Next, 2 μ L of iodoacetamide (1 M) was added and incubated for 1 hour at room temperature in the dark. Subsequently, 80 μ L of the proteolytic buffer was added (Trypsin buffer: 50 mM Ambic pH 8.5, 5% acetonitrile; Chymotrypsin buffer: Tris HCl 100 mM, CaCl₂ 10 mM pH 7.8; ASP-N buffer: Phosphate buffer 50 mM pH 7.8; Elastase buffer: Tris HCl 50 mM pH 8.0; Thermolysin buffer: Tris HCl 50 mM, CaCl₂ 0.5 mM pH 9.0). 100 μ L of the reduced/alkylated antigen was mixed with trypsin (Roche Diagnostic), chymotrypsin

(Roche Diagnostic), ASP-N (Roche Diagnostic), elastase (Roche Diagnostic), or thermolysin (Roche Diagnostic) at the ratio 1/50–1/200 (w/w). The proteolytic mixture was incubated overnight at 25–70°C.

Data acquisition was achieved with a nano-liquid chromatography system (Ultimate 3000-RSLC) coupled with high-resolution Q-Exactive MS (Thermo Scientific) with a 300- μ m ID x 5-mm C18 PepMapTM column using top 12 DDA mode. Gradient is 4–40% B in 48 min with mobile phase A as 95/05/0.1 H₂O/ACN/HCOOH and mobile phase B as 20/80/0.1 H₂O/ACN/HCOOH.

The cross-linked peptides were analyzed using XQuest (Y.J. Lee, Mol. BioSyst., 2008, 4, 816–823) and Stavrox³⁵ with precursor mass tolerance of 10 ppm, fragment mass tolerance of 0.02 Da, and S/N threshold of 1.5 in FT mode. Only positive cross-link observed with both software and in triplicate analysis were reported.

Acknowledgments

Ryan Wenzel from CovalX (Saugus, MA, USA), John Schenkel and Mark Chance from NEO Proteomics, Inc. (Cleveland, OH, USA) and Jennifer Pawlowski of Merck & Co., Inc., Kenilworth, NJ, USA for editorial support.

Disclosure statement

D.L. Hulsik and J. Kreijtz are employed by, and may own stock in, Aduro Biotech Europe who partially provided funding for this study and own stock in Chinook Therapeutics (KDNY). A. Beebe, X. Dang, M. Beaumont, E. Hsieh, G. Ermacov, T. Fischmann, and V. Juan, are employed by, and may own stock in, Merck & Co., Inc., Rahway, NJ, USA, who partially provided funding for this study. A. Nazabal is employed by, and may own stock in, CovalX, Inc, who provided chemical cross-linking data for this study. L. Guelen and H.v. Eenennaam hold patents in Merck Sharpe & Dohme Corp and own Chinook stock.

Funding

Merck Sharp & Dohme Corp. LLC, a subsidiary of Merck & Co., Inc., Rahway, NJ, USA and Aduro Biotech Europe B.V.

References

- Grilo AL, Mantalaris A. The increasingly human and profitable monoclonal antibody market. *Trends Biotechnol.* 2019;37(1):9–16. doi:10.1016/j.tibtech.2018.05.014.
- Mullard A. FDA approves 100th monoclonal antibody product. *Nat Rev Drug Discov.* 2021;20(7):491–95. doi:10.1038/d41573-021-00079-7.
- Sukumar S, Wilson DC, Yu Y, Wong J, Naravula S, Ermakov G, Riener R, Bhagwat B, Necheva AS, Grein J, et al. Characterization of MK-4166, a clinical agonistic antibody that targets human GITR and inhibits the generation and suppressive effects of T regulatory cells. *Cancer Res.* 2017;77(16):4378–88. 1439.2016. doi:10.1158/0008-5472.CAN-16-1439.
- van Meerten T, Rozemuller H, Hol S, Moerer P, Zwart M, Hagenbeek A, Mackus WJM, Parren PWI, van de Winkel JGJ, Ebeling SB, et al. HuMab-7D8, a monoclonal antibody directed against the membrane-proximal small loop epitope of CD20 can effectively eliminate CD20low expressing tumor cells that resist Rituximab mediated lysis. *Haematologica.* 2010;95(12):2063–71. haematol.2010.025783. doi:10.3324/haematol.2010.025783.
- He W, Tan GS, Mullarkey CE, Lee AJ, Lam MMW, Krammer F, Henry C, Wilson PC, Ashkar AA, Palese P, et al. Epitope specificity

- plays a critical role in regulating antibody-dependent cell-mediated cytotoxicity against influenza A virus. *Proc Natl Acad Sci USA.* 2016;113(42):11931. doi:10.1073/pnas.1609316113.
- de Goeij BECG, Peipp M, de Haij S, van den Brink EN, Kellner C, Riedl T, de Jong R, Vink T, Strumane K, Bleeker WK, et al. HER2 monoclonal antibodies that do not interfere with receptor heterodimerization-mediated signaling induce effective internalization and represent valuable components for rational antibody-drug conjugate design. *MABs.* 2014;6(2):392–402. doi:10.4161/mabs.27705.
 - Deng X, Storz U, Doranz BJ. Enhancing antibody patent protection using epitope mapping information. *MABs.* 2018;10(2):204–09. doi:10.1080/19420862.2017.1402998.
 - Accchione M, Lipschultz CA, DeSantis ME, Shanmuganathan A, Li M, Wlodawer A, Tarasov S, Smith-Gill SJ. Light chain somatic mutations change thermodynamics of binding and water coordination in the HyHEL-10 family of antibodies. *Mol Immunol.* 2009;47(2–3):457–64. doi:10.1016/j.molimm.2009.08.018.
 - Gribenko AV, Parris K, Mosyak L, Li S, Handke L, Hawkins JC, Severina E, Matsuka YV, Anderson AS. High resolution mapping of bactericidal monoclonal antibody binding epitopes on *Staphylococcus aureus* antigen MntC. *PLoS Pathog.* 2016;12(9):e1005908. doi:10.1371/journal.ppat.1005908.
 - Garman EF. Developments in X-ray crystallographic structure determination of biological macromolecules. *Sci.* 2014;343(6175):1102. doi:10.1126/science.1247829.
 - Zhang M, Huang R, Beno B, Deyanova E, Li J, Chen G, Gross M. Epitope and paratope mapping of PD-1/Nivolumab by mass spectrometry-based Hydrogen–deuterium exchange, cross-linking, and molecular docking. *Anal Chem.* 2020;92(13):9086–94. doi:10.1021/acs.analchem.0c01291.
 - Abbott WM, Damschroder MM, Lowe DC. Current approaches to fine mapping of antigen–antibody interactions. *Immunology.* 2014;142(4):526–35. doi:10.1111/imm.12284.
 - Liu X, Huang R, Zhao F, Chen G, Tao L. Advances in mass spectrometry-based epitope mapping of protein therapeutics. *J Pharmaceut Biomed.* 2022;215:114754. doi:10.1016/j.jpba.2022.114754.
 - Leitner A. Cross-linking and other structural proteomics techniques: how chemistry is enabling mass spectrometry applications in structural biology. *Chem Sci.* 2016;7(8):4792–803. doi:10.1039/C5SC04196A.
 - Lee JY, Lee HT, Shin W, Chae J, Choi J, Kim SH, Lim H, Won Heo T, Park KY, Lee YJ, et al. Structural basis of checkpoint blockade by monoclonal antibodies in cancer immunotherapy. *Nat Commun.* 2016;7(1):13354. doi:10.1038/ncomms13354.
 - Ramagopal UA, Liu W, Garrett-Thomson SC, Bonanno JB, Yan Q, Srinivasan M, Wong SC, Bell A, Mankikar S, Rangan VS, et al. Structural basis for cancer immunotherapy by the first-in-class checkpoint inhibitor ipilimumab. *Proc Natl Acad Sci USA.* 2017;114(21):E4223. doi:10.1073/pnas.1617941114.
 - Bai A, Meetze K, Vo N, Kollipara S, Mazsa E, Winston W, Weiler S, Poling L, Chen T, Ismail N, et al. GP369, an FGFR2-IIIb-Specific antibody, exhibits potent antitumor activity against human cancers driven by activated FGFR2 signaling. *Cancer Res.* 2010;70(19):7630–39. doi:10.1158/0008-5472.CAN-10-1489.
 - Wang C, Thudium K, Han M, Wang X, Huang H, Feingersh D, Garcia C, Wu Y, Kuhne M, Srinivasan M, et al. In vitro characterization of the anti-PD-1 antibody nivolumab, BMS-936558, and in vivo toxicology in non-human primates. *Cancer Immunol Res.* 2014;2(9):846–56. doi:10.1158/2326-6066.CIR-14-0040.
 - Guadagnoli M, Kimberley FC, Phan U, Cameron K, Vink PM, Rodermond H, Eldering E, Kater AP, van Eenennaam H, Medema JP, et al. Development and characterization of APRIL antagonistic monoclonal antibodies for treatment of B-cell lymphomas. *Blood.* 2011;117(25):6856–65. doi:10.1182/blood-2011-01-330852.
 - <https://nationalmaglab.org/user-facilities/icr/techniques/hd-exchange>.

21. Alverdi V, Mazon H, Versluis C, Hemrika W, Esposito G, van den Heuvel R, Scholten A, Heck AJR. cGMP-binding prepares PKG for substrate binding by disclosing the C-terminal domain. *J Mol Biol.* 2008;375(5):1380–93. doi:10.1016/j.jmb.2007.11.053.
22. Huang W, Ravikumar K, Chance M, Mark R, Yang S. Quantitative mapping of protein structure by hydroxyl radical footprinting-mediated Structural mass spectrometry: a protection factor analysis. *Biophys J.* 2015;108(1):107–15. doi:10.1016/j.bpj.2014.11.013.
23. Maleknia SD, Downard KM. Radical approaches to probe protein structure, folding, and interactions by mass spectrometry. *Mass Spectrom Rev.* 2001;20(6):388–401. doi:10.1002/mas.10013.
24. Merkley ED, Rysavy S, Kahraman A, Hafen RP, Daggett V, Adkins JN. Distance restraints from crosslinking mass spectrometry: mining a molecular dynamics simulation database to evaluate lysine–lysine distances. *Protein Sci.* 2014;23(6):747–59. doi:10.1002/pro.2458.
25. Rand KD, Zehl M, Jørgensen TJD. Measuring the Hydrogen/Deuterium Exchange of Proteins at High Spatial Resolution by Mass Spectrometry: Overcoming Gas-Phase Hydrogen/Deuterium Scrambling. *Acc Chem Res.* 2014;47(10):3018–27. doi:10.1021/ar500194w.
26. Hamuro Y, E SY. Determination of backbone amide hydrogen exchange rates of cytochrome c using partially scrambled electron transfer dissociation data. *J Am Soc Mass Spectrom.* 2018;29(5):989–1001. doi:10.1007/s13361-018-1892-3.
27. Brodie NI, Huguet R, Zhang T, Viner R, Zabrouskov V, Pan J, Petrotchenko EV, Borchers CH. Top-down Hydrogen–deuterium exchange analysis of protein structures using ultraviolet photodissociation. *Anal Chem.* 2018;90(5):3079–82. doi:10.1021/acs.analchem.7b03655.
28. Schmitz C, Melquiond AS, de Vries SJ, Karaca E, van Dijk M, Kastiris PL, Bonvin AM. Protein–Protein Docking with HADDOCK. *NMR Of Biomolecules.* 2012;520–535. doi:10.1002/9783527644506.ch32.
29. Zhang Y, Rempel DL, Zhang H, Gross ML. An improved fast photochemical oxidation of proteins (FPOP) platform for protein therapeutics. *J Am Soc Mass Spectrom.* 2015;26(3):526–29. doi:10.1007/s13361-014-1055-0.
30. Chance MR, Farquhar ER, Yang S, Lodowski DT, Kiselar J. Protein footprinting: auxiliary engine to power the Structural biology revolution. *J Mol Biol.* 2020;432(9):2973–84. doi:10.1016/j.jmb.2020.02.011.
31. Meyerson JR, Kumar J, Chittori S, Rao P, Pierson J, Bartesaghi A, Mayer ML, Subramaniam S. Structural mechanism of glutamate receptor activation and desensitization. *Nature.* 2014;514(7522):328. <https://www.nature.com/articles/nature13603#supplementary-information>.
32. Bardelli M, Livoti E, Simonelli L, Pedotti M, Moraes A, Valente AP, Varani L. Epitope mapping by solution NMR spectroscopy. *J Of Molecular Recognition.* 2015;28(6):393–400. doi:10.1002/jmr.2454.
33. Monaco S, Tailford LE, Juge N, Angulo J. Differential epitope mapping by STD NMR spectroscopy to reveal the nature of protein–ligand contacts. *Angew Chem Int Ed.* 2017;56(48):15289–93. doi:10.1002/anie.201707682.
34. Renaud J-P, Chari A, Ciferri C, Liu W-T, Rémy H-W, Stark H, Wiesmann C. Cryo-EM in drug discovery: achievements, limitations and prospects. *Nat Rev Drug Discov.* 2018;17(7):471–92. doi:10.1038/nrd.2018.77.
35. Götze M, Pettelkau J, Schaks S, Bosse K, Ihling CH, Krauth F, Fritzsche R, Kühn U, Sinz A. StavroX—A software for analyzing crosslinked products in protein interaction studies. *J Am Soc Mass Spectrom.* 2012 Jan;23(1):76–87. doi:10.1007/s13361-011-0261-2.